IJRAR.ORG E-ISSN: 2348-1269, P-ISSN: 2349-5138

INTERNATIONAL JOURNAL OF RESEARCH AND ANALYTICAL REVIEWS (IJRAR) | IJRAR.ORG

An International Open Access, Peer-reviewed, Refereed Journal

# Design and Analysis of LCL Filters for Smart Grid-Integrated Three-Phase Power Converters with IoT-Enabled Monitoring

**Saurabh kumar**
Electrical Engineering
JIS College of Engineering
Kalyani, WB, India

**Dr. Alok Kumar Shrivastav**
H.O.D
Electrical Engineering
JIS College of Engineering
Kalyani, WB, India

**Shivam Kumar**
Electrical Engineering
JIS College of Engineering
Kalyani, WB, India

**Nirbhay Kumar**
Electrical Engineering
JIS College of Engineering
Kalyani, WB, India

**Kusum Singh**
Electrical Engineering
JIS College of Engineering
Kalyani, WB, India

**Abstract**

The use of power converters to integrate renewable energy sources with the AC grid has significantly increased over the past two decades. To connect these converters to the utility grid while effectively filtering the high-order harmonics they generate, LCL filters are commonly employed. Achieving high filtering performance that complies with stringent grid code requirements, while also balancing cost and efficiency, necessitates an optimal design of the LCL filter. This paper presents the modeling and a comprehensive design methodology for an LCL filter used in grid-connected converters, based on an analytical approach. The design process carefully selects the inverter-side inductor, grid-side inductor, and filter capacitor to ensure effective harmonic attenuation, minimize resonance issues, and maintain system stability. Simulation results demonstrate that the proposed design method successfully mitigates approximately 98.51% of the current harmonics present at the converter output, highlighting its effectiveness in improving power quality and ensuring compliance with grid standards.

**Keywords:** LCL Filter, Power Converter, Total Harmonic Distortion (THD), Passive Damping.

## 1.0 Introduction

The use of power converters to interconnect with the grid has been increasing in applications such as power quality improvement, regenerative motor drives, and distributed generation (DG) (John et al., 2009). Various distributed generation systems like photovoltaic (PV) and fuel cells produce energy in the form of DC voltage sources. Moreover, wind energy often produces variable AC, which is frequently converted to DC as well. When interfaced with a DC/AC inverter, these DG systems can supply energy into the utility grid. However, the power electronic devices used in these voltage source inverters (VSI) inject undesirable harmonics that affect nearby loads at the point of common coupling (PCC) with the utility grid, potentially breaching typical standards for grid interconnection.

Hence, to interface these power converters (VSIs) to the utility grid, filters are often required to reduce harmonics in the output current to acceptable limits (Sarkar, 2015). Among the various filter types, the LCL filter is recognized as one of the best performing for grid-connected voltage source inverters (Jayalath and Hanif, 2017b). Designing filters for grid-connected inverter applications involves numerous constraints. The filter requirements are driven by stringent standards such as IEEE 519-1992 – IEEE Recommended Practices and Requirements for Harmonic Control in Electrical Power Systems, IEEE 1547.2-2008 – IEEE Application Guide for IEEE Standard, and IEEE 1547-2005 – IEEE Standard for Interconnecting Distributed Resources with Electric Power Systems (John et al., 2009; IEEE Standard 519 – 1992, 1993; IEEE Standard 1547.1 – 2005, 2005). Additional design considerations include reactive power compensation limits and maximum allowable voltage drop across the filter to limit switching losses (John et al., 2009; Jayalath and Hanif, 2017b). Higher-order LCL filters are essential to achieve these regulatory requirements while maintaining a compact size and weight (John et al., 2009). The design of LCL filter parameters—specifically the grid-side and inverter-side inductors and the capacitor—typically follows an iterative approach due to the interdependence of filter parameters and design requirements (Jayalath and Hanif, 2017a). The objective of this paper is to propose design procedures for such higher-order LCL filters and to provide insights into methodologies for optimized filter design.

### 1.1 Advantage of High order Filter over First order Filter

A simple first-order L filter, while straightforward in design, is not only bulky but also fails to meet the stringent specifications required for harmonic attenuation in modern grid-connected inverters (Channegowda et al., 2010). In contrast, the adoption of a third-order LCL filter has become common practice, as it achieves significantly higher attenuation of harmonics and allows for a notable reduction in both the size and cost of filter components (Karshenas and Saghafi, 2006; Liserre et al., 2005; Channegowda et al., 2010)268.

However, designing an LCL filter systematically is a complex task due to the interdependence of various parameters (Jayalath and Hanif, 2017a)6. Key factors that must be carefully considered include the output current ripple, harmonics generated by switching devices such as IGBTs, the series fundamental voltage drop, desired power factor, resonance frequency, and overall control stability (Liserre et al., 2005; Channegowda et al., 2010)28. Additionally, attention to the overall filter size and cost is essential for achieving an efficient and practical design.

Comparative analysis, as illustrated in Figure 1, shows that a third-order LCL filter provides superior attenuation of higher harmonic frequencies than a first-order L filter. For the same or even lower net inductance (L1+L2), the LCL filter achieves much better attenuation—up to 60 dB/decade—at frequencies above its resonance point. This makes the LCL filter highly effective for meeting modern grid codes and power quality standards while optimizing system size and cost268.

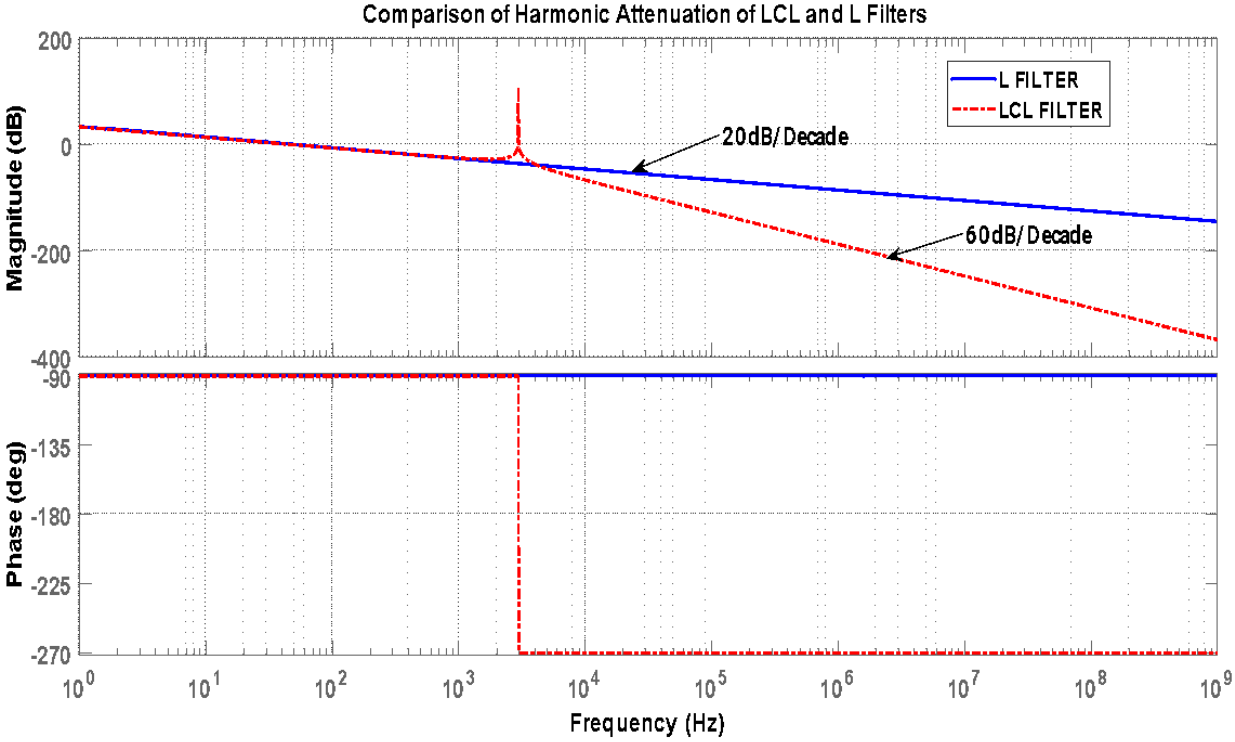


Figure 1: Comparison of Harmonic Attenuation of LCL and L Filters

## 2.0 Characterization of Harmonics in PV Inverter System

The level and order of harmonics present in the output of a Voltage Source Inverter (VSI) is determined. The characterization is done to know the level of harmonics that is present in the output of a VSI.

Here, the Voltage Source Inverter (VSI) was implemented in a Simulink window and the output of the VSI is analyzed in terms of the harmonic content and distortion in the current waveform. Figure 2 shows the Simulink model for the characterization.

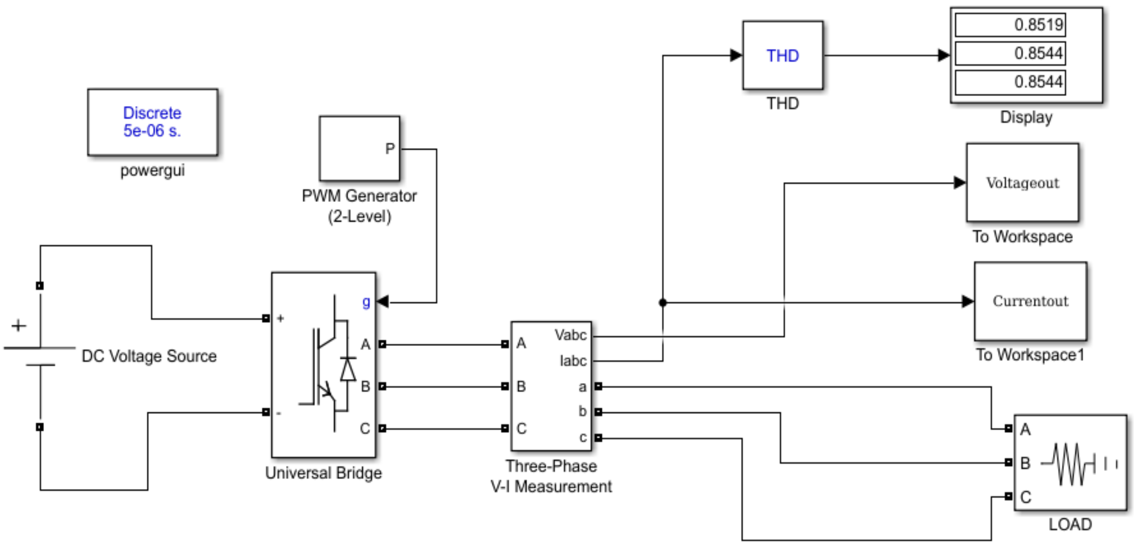


Figure 2: Simulink Model for Characterization of Harmonics in PV Inverter System

### 2.1 Modeling and Design of LCL Filter

The transfer function model of the LCL filter is developed and the parameters of the model gotten through a clear design procedure. The modeling and the design of the LCL filter are done to determine the values of the parameters of the filter. The LCL filter is used to mitigate higher order harmonics present at the output of the VSI. A mathematical model is developed using the power circuit of a three phase grid connected VSI with LCL filter. The three phase power circuit is reduced to a single phase equivalent circuit and the transfer function of the LCL filter derived using the circuit parameters.

#### 2.1.1 LCL Filter Mathematical Model

The power circuit of a three phase grid connected power converter is presented in Figure 3. As depicted in this figure and in the Single Phase equivalent circuit of Figure 4, the LCL filter is used to interface between the grid and the power converter. Vg refers to the grid voltage, while $L_1$and $L_2$ are the converter side inductor of the LCL filter and the grid side inductor of the LCL filter respectively. C refers to the LCL filter capacitor and $R_D$ is the damping resistor. $V_{DC}$ is the DC – Bus Voltage.

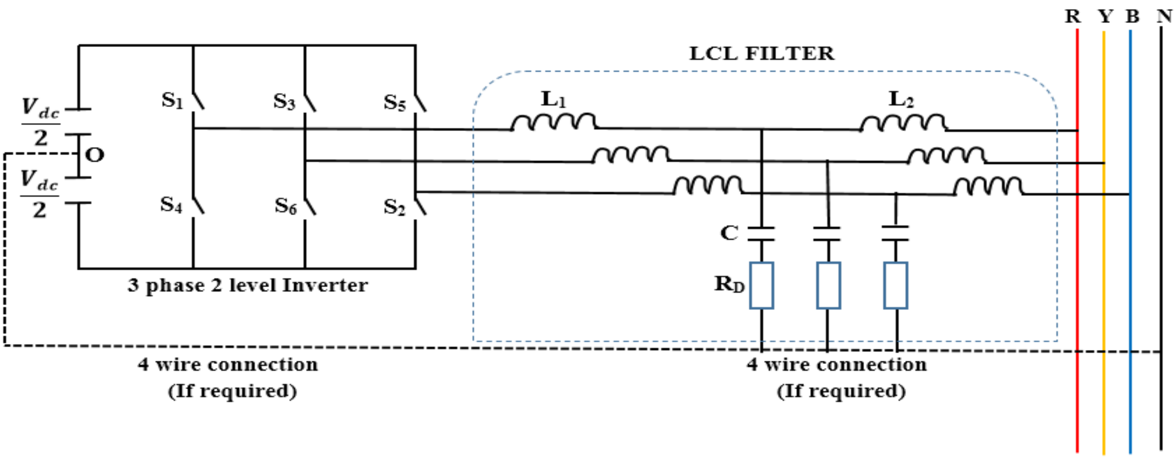


Figure 3: Power circuit of the three phase grid connected Inverter with LCL filter

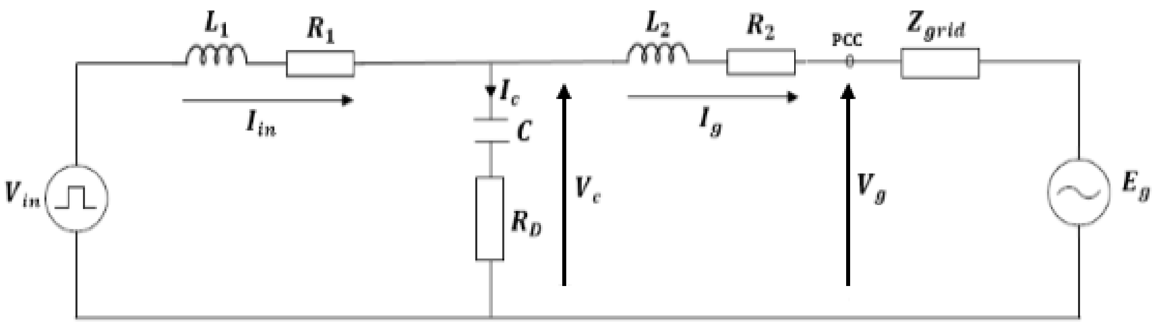


Figure 4: Single Phase equivalent circuit

In the model of the LCL filter, we consider that;

- At frequencies other than the fundamental frequency, the grid behaves essentially as a short circuit, i.e. Vg = 0.

An important transfer function for the LCL filter is given as;

$$H = \frac{i_g}{V_{in}} = \frac{Filter\ output\ current}{input\ voltage} \quad (2.1)$$

Therefore, $H$ is an admittance transfer function and in the complex $S$ domain, we have;

$$H(s) = \frac{I_g(s)}{V_{in}(s)} \quad (2.2)$$

Applying Kirchhoff's laws, the equivalent circuit in Figure 4, the mathematical model of the filter in s-plane is given by these equations:

$$I_{in} - I_c - I_g = 0 \quad (2.3)$$

$$V_{in} - V_c = I_{in}(sL_1 + R_1) \qquad (2.4)$$

$$V_c - V_g = I_g(sL_2 + R_2) \qquad (2.5)$$

$$V_c = I_c\left(\frac{1}{sC} + R_D\right) \qquad (2.6)$$

The circuit parameters are defined as;

| | |
|---|---|
| $V_{in}$ | Inverter Voltage |
| $I_{in}$ | Inverter Current |
| $V_c$ | Voltage across Filter Capacitor |
| $I_c$ | Filter Capacitor Current |
| $I_g$ | Grid Current |
| $L_1$ | Inverter side inductor |
| $L_2$ | Grid side inductor |
| C | Capacitor |
| $R_D$ | Damping Resistor |
| $V_g$ | Grid voltage |
| $R_1$ | Inverter Side Parasitic Resistance |
| $R_2$ | Grid Side Parasitic Resistance |

Figure 5 gives the block diagram of the LCL Filter in the frequency domain.

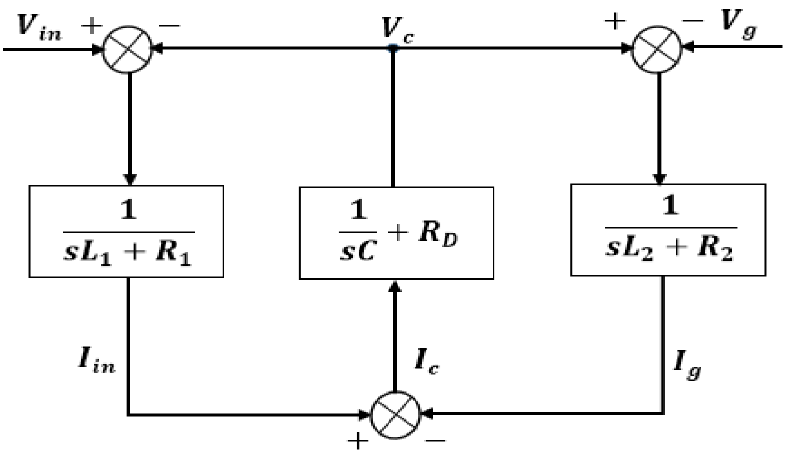


Figure 5: Block diagram of LCL Filter in S – Plane

Recall that for frequencies other than the fundamental frequency, Vg = 0.

Putting Vg = 0 in equation 2.5, gives;

$$V_c = I_g(sL_2 + R_2) \qquad (2.7)$$

Equating 2.6 with 2.7 yields;

$$I_g(sL_2 + R_2) = I_c\left(\frac{1}{sC} + R_D\right) \qquad (2.8)$$

*This implies that;*

$$I_c = I_g\left(\frac{s^2CL_2 + sCR_2}{sCR_D + 1}\right) \qquad (2.9)$$

From equation 2.3,

$$I_{in} = I_c + I_g \qquad (2.10)$$

Putting equation 2.9 into equation 2.10 gives;

$$I_{in} = I_g + I_g\left(\frac{s^2CL_2 + sCR_2}{sCR_D + 1}\right) \qquad (2.11)$$

Also, from equation 2.4,

$$V_{in} = V_c + I_{in}(sL_1 + R_1) \qquad (2.12)$$

Substituting equations 2.7 and 2.11 into 2.12 gives;

$$V_{in} = I_g(sL_2 + R_2) + (sL_1 + R_1)\left[I_g + I_g\left(\frac{s^2CL_2 + sCR_2}{sCR_D + 1}\right)\right] \qquad (2.13)$$

$$V_{in} = I_g\left[(sL_1 + R_1) + (sL_2 + R_2) + \frac{(sL_1 + R_1)(s^2CL_2 + sCR_2)}{sCR_D + 1}\right] \qquad (2.14)$$

$$V_{in} = I_g\left[\frac{s^3CL_1L_2 + s^2C(L_1(R_2 + R_D) + L_2(R_1 + R_D)) + s\big(L_1 + L_2 + C(R_1R_2 + R_1R_D + R_2R_D)\big) + R_1 + R_2}{sCR_D + 1}\right] \qquad (2.15)$$

Therefore, the transfer function according to equation 2.2 is:

$$Hd_{LCL}(s) = \frac{sCR_D + 1}{s^3CL_1L_2 + s^2C(L_1(R_2 + R_D) + L_2(R_1 + R_D)) + s\big(L_1 + L_2 + C(R_1R_2 + R_1R_D + R_2R_D)\big) + R_1 + R_2} \qquad (2.16)$$

Without the damping resistance $R_D$, equation 2.16 becomes;

$$H_{LCL}(s) = \frac{1}{s^3CL_1L_2 + s^2C(L_1R_2 + L_2R_1) + s\big(L_1 + L_2 + C(R_1R_2)\big) + R_1 + R_2} \qquad (2.17)$$

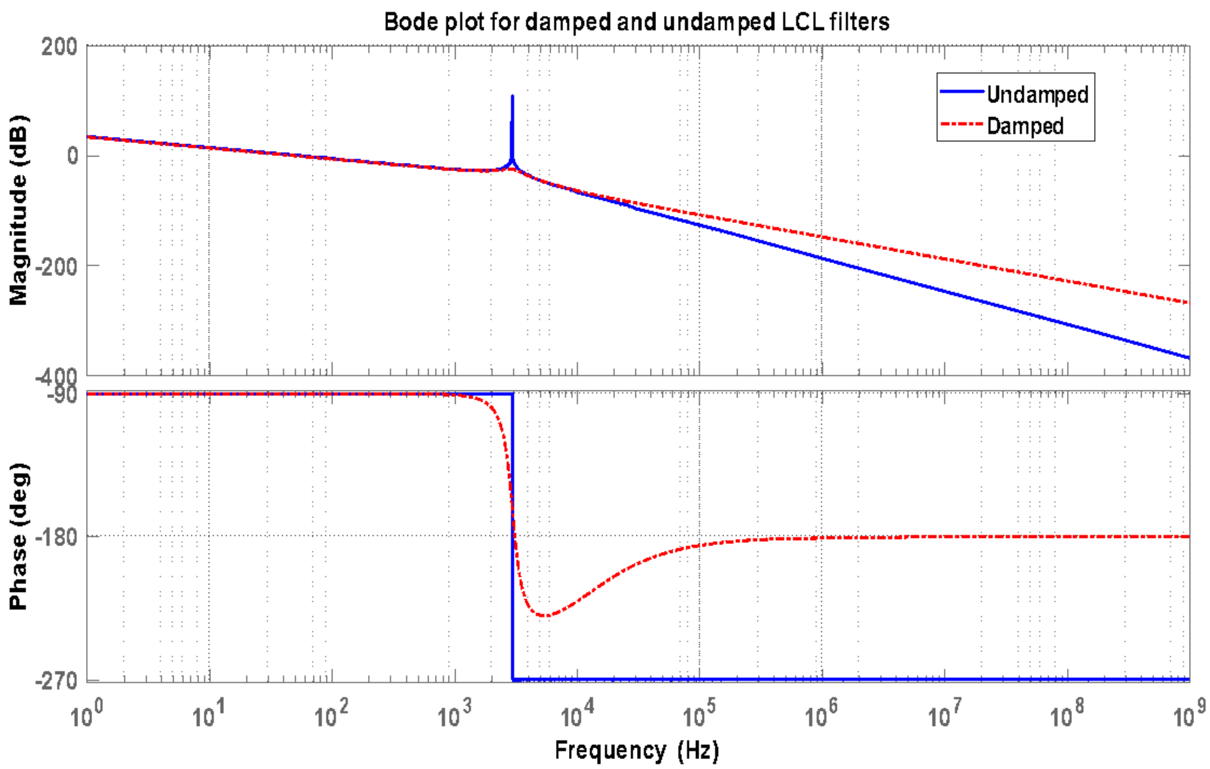


Figure 6: Bode plot for damped and undamped LCL filters

The Bode plots of the LCL filter without and with damping are shown in Figure 3.6. The insertion of a series resistance with the capacitor eliminates the gain spike, smoothing the overall response and rolling-off to -180 degrees for high frequency, instead of - 270 degrees. The LCL filter can achieve high performance at high frequency with an attenuation rate of -60 dB/decade.

## 2.2 LCL Filter Design Procedure

The LCL filter design methodology is aimed to meet grid code requirements through efficient attenuation of high order current harmonic components on the grid side. It requires the following nominal system parameters. Table 1 shows the nominal system parameters used in the design.

Base Values:

$$Base\ voltage = V_B = E_n = \sqrt{3} \times V_g = \sqrt{3} \times 240 = 415V$$

$$Base\ Impedance = Z_B = \frac{{E_n}^2}{P_n} = \frac{415^2}{100000} = 1.7223\Omega$$

$$Base\ angular\ frequency = \omega_g = 2\pi f_g = 2\pi \times 50 = 314.2\ rads$$

$$Base\ Capacitance = C_B = \frac{1}{\omega_g Z_B} = \frac{1}{314.2 \times 1.7223} = 1847.93\mu F$$

$$Base\ Inductance = L_B = \frac{Z_B}{\omega_g} = \frac{1.7223}{314.2} = 5.482mH$$

Any quantity when divided by its base value is expressed in p.u. (per unit)

Important Ratios:

- Ratio between the LCL filter inductances, otherwise called split factor

$$r_l = \frac{L_2}{L_1} \tag{2.18}$$

- Ratio between the LCL filter capacitance and total inductance in p.u.

$$r_q = \frac{c}{l_T} = \frac{{Z_B}^2 C}{L_T} \tag{2.19}$$

- Ratio between the switching and resonance frequency

$$r_f = \frac{f_{sw}}{f_{res}} = \frac{\omega_{sw}}{\omega_{res}} \tag{2.20}$$

### 2.2.1 LCL Filter Design Criteria

The following are some important design criteria for the LCL filter.

- Fulfillment of reactive volt-ampere (VAR) limits (power factor nearly equal to 1)
- Optimal volume and weight with resulting minimum cost of passive (inductive and capacitive) components
- Attenuation of higher order harmonics from the output current (THD≤ 0.03)
- Proper choice of resonance frequency such that the switching harmonics are sufficiently attenuated and the size of the filter components is not too large (Sarkar, 2015; Karshenas and Saghafi, 2006; Ben Said-Romdhane *et al.*, 2017) ($10f_g \le f_{res} \le 0.5f_{sw}$).

### 2.2.2 Inverter side Inductance Design

For the first step, we have to design the inverter side inductance. To do this, the approach propose by (Reznik *et al.*, 2013) is adopted.

Here, we consider the maximum current ripple present at the output of an inverter which is given as;

$$\Delta I_{Lmax} = \frac{2V_{DC}}{3L_1}(1-m)mT_{sw} \quad (2.21)$$

Where m is modulation index and $T_{sw} = \frac{1}{f_{sw}}$

But, maximum peak to peak current ripple occurs when m is 0.5. Thus, equation 2.21 becomes;

$$\Delta I_{Lmax} = \frac{V_{DC}}{6f_{sw}L_1} \quad (2.22)$$

Considering a 10% ripple of the rated current for the design parameters, equation 2.21 is given by:

$$\Delta I_{Lmax} = 0.1I_{max} \quad (2.23)$$

Where;

$$I_{max} = \frac{\sqrt{2}P_n}{3V_{ph}} \quad (2.24)$$

$$L_1 = \frac{V_{DC}}{6f_{sw}\Delta I_{Lmax}} \quad (2.25)$$

From equation 2.25, we have;

$$L_1 = \frac{800}{6 \times 16000 \times 19.642} = 0.424mH$$

### 2.2.3 Maximum LCL Filter Capacitor Value

A lesser value of the filter capacitor C will reduce unnecessary flow of larger reactive currents through it. We know that the flow of reactive power is tied to voltage stability. Therefore, a larger value of C can introduce voltage instability problems in the grid. In this case, the LCL filter capacitor C is designed so that its consumption of reactive power is less than n% of the rated power $P_n$ as shown in Equation (3.26a) (Ben Said-Romdhane *et al.*, 2017). In this equation, $Q_c$ denotes the reactive power consumed by the filter capacitor and n is a positive factor chosen and is generally equal to or less than 5% (Sarkar, 2015; Ben Said-Romdhane *et al.*, 2017). According to Equations (2.26a) and (2.26b), the maximum value of the filter capacitor can be expressed as in Equation (2.26c):

$$Q_C = n\%.P_n \quad 2.26a$$

But,

$$Q_C = -{E_n}^2 C\omega_g \quad 2.26b$$

This implies that for n = 5%,

$$C_{max} = 0.05\left(\frac{P_n}{3{V_g}^2\omega_g}\right) \quad 2.26c$$

$$C_{max} = 92.4\mu F$$

In this case, C = $C_{max}$ and is exactly 5% of the base capacitance $C_B$.

### 2.2.4 Grid side Inductance Design

To obtain a ripple attenuation of 20% on the grid side with respect to the current ripple on the inverter side.

$$L_2 = \frac{\sqrt{\frac{1}{k^2}} + 1}{C{f_{sw}}^2} \qquad (2.27)$$

The attenuation factor k in equation 2.27 is set to a value of 20% (0.2).

$$L_2 = \frac{\sqrt{\frac{1}{0.2^2}} + 1}{92.4 \times 10^{-6} \times 16000^2} = 0.254mH$$

### 2.2.5 Resonance Frequency Design

The resonance frequency depends on the filter inductors $L_1$ and $L_2$ and the filter capacitor C.

Let $L = L_1 + L_2$ $and$ $L_p = \frac{L_1 L_2}{L_1 + L_2}$

But generally for any given tank circuit, $\omega_{res} = \frac{1}{\sqrt{LC}}$

Thus, for the LCL filter,

$$\omega_{res} = \frac{1}{\sqrt{L_p C}} \qquad 2.28$$

Also, the calculated value of $\omega_{res}$ must satisfy the inequality given in equation 2.29. Otherwise, the values of equation 3.27 is re-chosen.

$$10f_g \le f_{res} \le 0.5f_{sw} \qquad (2.29)$$

Note that $\omega_{res}$ is in radians.

From equation 2.28;

$$\omega_{res} = \frac{1}{\sqrt{0.000158843 \times 92.4 \times 10^{-6}}} = 8254.29\, rads/sec$$

$$f_{res} = \frac{8254.29}{2\pi} = 1313.71Hz$$

In this case, $f_{res}$ is taken to be 1500Hz (i.e. $w_{res} = 9425\, rads/sec$) and this satisfies the inequality in equation 2.29.

### 2.2.6 Minimum DC Bus Voltage

According to Ben Said-Romdhane *et al.* (2017), For Voltage source converter, the DC-bus voltage will decide the maximum AC voltage that can be generated. A general guideline will be that the minimum DC voltage should be equal to the maximum line-to-line voltage of the grid. For three-phase grid, this will be the peak value of the line-to-line voltage.

Thus,

$$V_{DCmin} = \sqrt{2}.V_L \qquad (2.30)$$

$V_L$ is the line-to-line voltage of the grid.

$$V_{DCmin} = 587V$$

In this design, $V_{DC}$ is 800V.

### 2.2.7 Damping Resistor Design

For this design, we consider a simple passive damping where a resistor $R_D$ is inserted in series with the capacitor to attenuate part of the ripple on the switching frequency in order to avoid resonance. According to Reznik *et al.* (2013), the value of this resistor should be one third of the impedance of the filter capacitor at the resonance frequency. That is;

$$R_D = \frac{1}{3\omega_{res}C} \tag{2.31}$$

$$R_D = \frac{1}{3 \times 238.73 \times 92.4 \times 10^{-6}} = 15\Omega$$

But Pena-Alzola *et al.* (2013), gives an expression for the minimum damping resistor $R_{Dmin}$. The authors revealed that for the system to be stable and in order to achieve a positive gain margin in the control of the system, the damping resistor value must comply with equation 2.32.

$$R_{Dmin} = \frac{1}{3} f_{sw} \left( \frac{{L_2}^2}{L_1 + L_2} \right) \tag{2.32}$$

$$R_{Dmin} = \frac{1}{3} \times 16000 \times 0.000095156 = 0.51\Omega$$

This means that the choice of $R_D$ should be such that it satisfies the relation;

$$0.51 \leq R_D \leq 15$$

Note: $R_1$ and $R_2$ are parasitic resistances of the inductors $L_1$ and $L_2$ respectively and their values can be chosen directly from the manufacturer's datasheet. In this case; $R_1 = 0.380\Omega$ and $R_2 = 0.162\Omega$.
Table 1 shows the design system parameters that will be used for the simulation.

### 2.2.8 Simulink Model of the Inverter System with the LCL Filter

Figure 7 shows the Simulink model of the Inverter system with the LCL filter. Here, the design parameters as shown in Table 1 was used to develop a Simulink model to carry out performance analysis on the LCL filter.

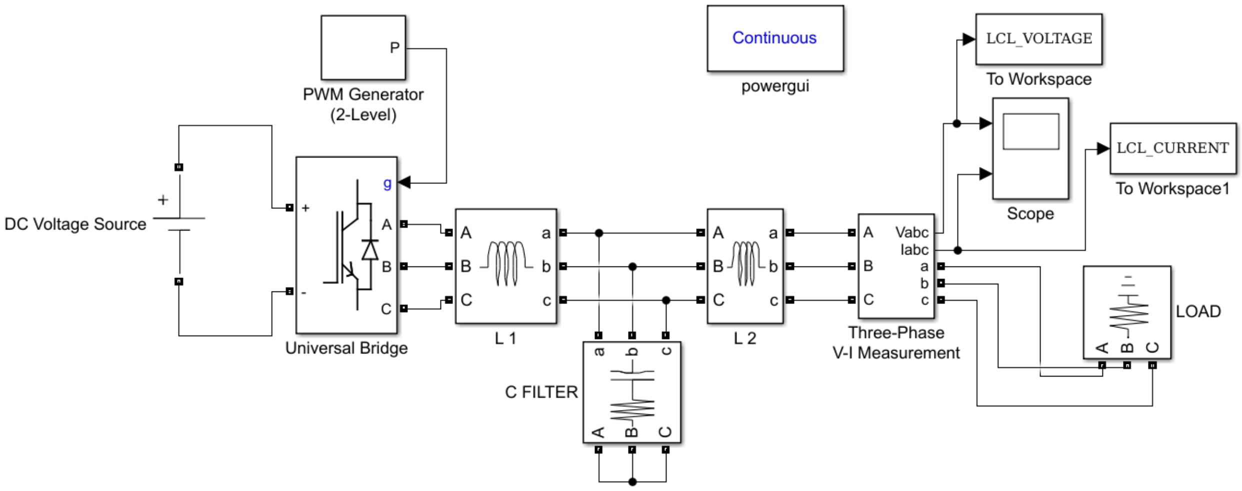


Figure 7: Simulink Model of the Inverter System with the LCL Filter

## 3.0 Results and Discussion

### 3.1 Harmonics in the PV Inverter System

In this section, the harmonic content in the unfiltered PV inverter system is presented. The current waveform and the Fast Fourier Transform (FFT) analysis are considered. From Figure 8 (a), it is seen that the current waveform is actually far from being sinusoidal due to very high content of harmonics. Figure 8 (b) gives the FFT analysis of this system, the Total Harmonic Distortion (THD) is as high as 85.17%, making it impossible and unsuitable for grid connected application. Utility operators accept a THD of less than 5% for all grid connected systems.

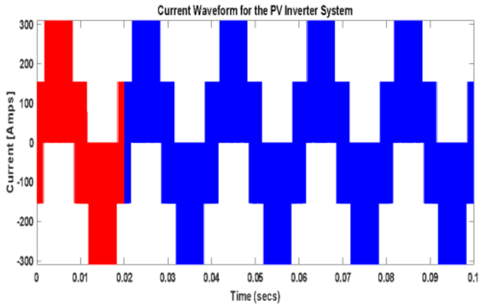


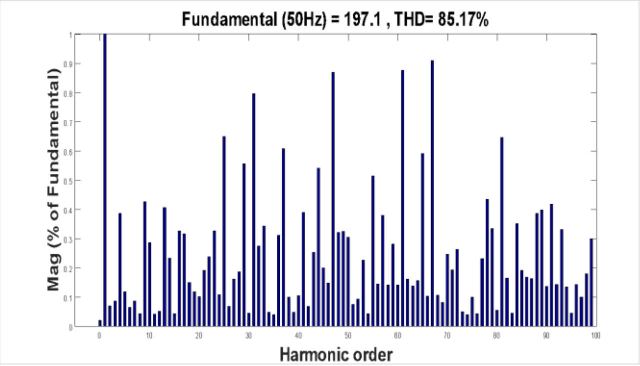


(a) Current waveform of the PV Inverter System (b) FFT analysis of the PV Inverter System

Figure 8: Current Waveform and FFT analysis of the PV Inverter System

### 3.2 The PV Inverter System Simulation Parameters

The inverter system is simulated using the design parameters obtained in section 2. The nominal system parameters and the design parameters are given in table 1.

Table 1: Design System Parameters

| | | |
|---|---|---|
| $f_g$ | Grid frequency or fundamental frequency | 50Hz |
| $f_{sw}$ | PWM carrier frequency | 16KHz |
| $W_{res}$ | Resonance frequency | 9425 rads/sec |
| $P_n$ | Rated active power | 100KW |
| $E_n$ | Line to line RMS voltage | $\sqrt{3} \times 240V$ |
| $V_{DC}$ | DC Bus voltage | 800V |
| $L_1$ | Inverter side inductor | 0.424mH |
| $L_2$ | Grid side inductor | 0.254mH |
| $R_1$ | Inverter Side Parasitic Resistance | 0.380 Ω |
| $R_2$ | Grid Side Parasitic Resistance | 0.162 Ω |
| C | Capacitor | 92.4µF |
| $R_D$ | Damping Resistor | 2.2Ω |
| $V_g$ | Grid voltage | 240V |

### 3.3 Simulation Results of the LCL Filter

Figure 9 (a) shows the output current waveform of the inverter system with the LCL filter. Here, it is seen that the waveforms are all sinusoidal at this point since a greater percentage of the harmonics present at the output of the PV inverter system has been filtered out by the well-designed LCL filter. The harmonic content has also been reduced from 85.17% to 1.27%. However, Figure 9 (b) reveals that the LCL filter cannot optimally handle the low order harmonics, hence the need for a current controller. The current controller is needed to filter out the low order harmonics to make the PV inverter system meets utility 'Standard for Interconnecting Distributed Resources with Electric Power Systems'.

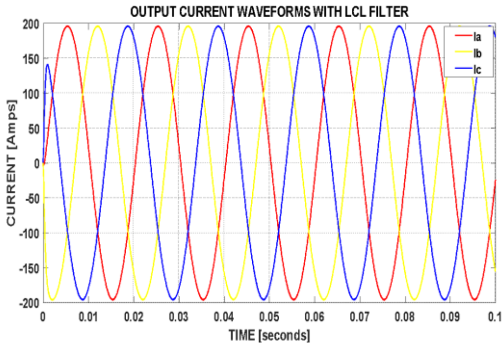


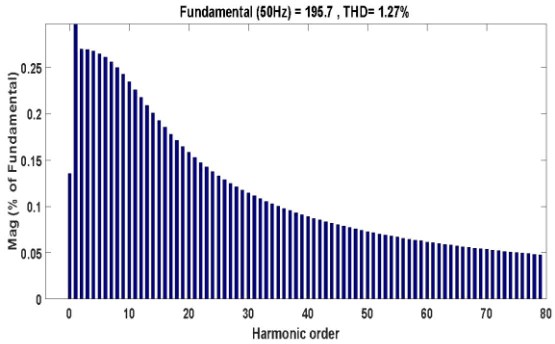


(a) Three – phase Output Current Waveforms with LCL Filter (b) FFT analysis of the PV Inverter System with LCL filter

Figure 9 : Current Waveforms and FFT of the Current of the Inverter System with LCL Filter

## 5. Conclusion

This paper proposes a simple, robust, and systematic design methodology for an LCL filter used to interface three-phase power converters with the utility grid, integrated within a smart IoT-enabled monitoring framework. The primary function of this filter is to reduce the switching frequency current harmonics generated by the power converter, thereby ensuring compliance with grid code requirements and improving power quality. The proposed methodology distinguishes itself from classical approaches by its simplicity and efficiency, offering a straightforward procedure that addresses key design criteria: fulfillment of reactive volt-ampere (VAR) limits, minimization of filter volume, achievement of total harmonic distortion (THD) $\leq 0.003$, and proper selection of resonance frequency.

In addition to the filter design, the integration of IoT technology enables real-time monitoring and remote diagnostics of the power converter and filter performance. This smart IoT-enabled system facilitates continuous data acquisition, fault detection, and predictive maintenance, enhancing the reliability and operational efficiency of grid-connected renewable energy systems.

The design process begins with determining essential system parameters such as grid voltage, rated power, grid frequency, and converter switching frequency. It then systematically tunes the LCL filter parameters—specifically the inverter-side and grid-side inductors, and the filter capacitor—while considering practical constraints like saturation current, component standard values, and resonance avoidance. This approach ensures that the filter meets harmonic attenuation requirements while remaining compact and cost-effective.

To validate the effectiveness of the proposed design, the obtained filter parameters were tested using MATLAB-Simulink software. Simulation results demonstrate the reliability, efficiency, and high filtering performance of the methodology, with over 98% of current harmonics at the converter output successfully mitigated. The integration of IoT further enables smart monitoring and control, making this approach well-suited for modern grid-connected converter applications that demand both high performance and intelligent system management.

**List of Symbols and Abbreviations Used**

Currents

| | |
|---|---|
| Ig | Grid Current |
| Ic | Filter Capacitor Current |

Voltages

| | |
|---|---|
| Vg | Grid Voltage |
| Vc | Voltage across Filter Capacitor |

Vin Inverter voltage
VB Base Voltage
VDC DC Link Voltage

Inductances
L1 Inverter Side Inductor
L2 Grid Side Inductor
LB Base Inductance

Resistances
R1 Inverter Side Parasitic Resistance
R2 Grid Side Parasitic Resistance
RD Damping Resistor

Impedances
ZB Base Impedance

Letters
S Laplace transform operator
F frequency [Hz]
L Inductor
LC Inductor Capacitor
C Capacitor
fsw Switching Frequency
fres Resonance Frequency
Pn Rated Active Power
En Line to Line RMS Voltage

Greek letters
ωres Resonance Frequency of the LCL filter in radians/sec

Acronyms
MATLAB Mathematics Laboratory
AC Alternating Current
DC Direct Current
FFT Fast Fourier Transform
RES Renewable Energy Sources
Kw Kilowatt
EMI Electromagnetic Interference
IEC International Electrotechnical Commission
PV Photovoltaic
DG Distributed Generation
VSI Voltage Source Inverter
KHz KiloHertz
IEEE Institute of Electrical and Electronics Engineers
THD Total Harmonic Distortion
LCL Inductor Capacitor Inductor

**References**


Ben Said-Romdhane, M.; Naouar, M.W.; Belkhodja, I. S.; Monmasson, E. (2017). "An Improved LCL Filter Design in Order to Ensure Stability without Damping and Despite Large Grid Impedance Variations," Energies 2017, 10, 336.

Channegowda, P. and John, V. (2010). "Filter optimization for grid interactive voltage Source Inverters," IEEE Trans. Ind. Electron., vol. 57, no. 12, pp. 4106-4114.

"519-1992 IEEE Recommended Practices and Requirements for Harmonic Control in Electrical Power Systems," IEEE Standard 519- 1992, 1993.

"1547.1 IEEE Standard Conformance Test Procedures for Equipment Interconnecting Distributed Resources with Electric Power Systems," IEEE Standard 1547.1-2005, 2005.

Jayalath, S. and Hanif, M. (2017a) "Generalized LCL – Filter Design Algorithm for Grid Connected Voltage Source Inverter," IEEE Transactions on Industrial Electronics 2017, pp. 1905 – 1915.

Jayalath S. and Hanif, M., (2017b). "An LCL – Filter Design with Optimal Total Inductance and Capacitance," IEEE Transactions on Power Electronics 2017, pp. 1 – 1. 10. 1109.

John, V.; Channegowda, P. B.; Mukherjee, N.; Krishnan, A. and Karanth, A. (2009). "Optimization of Higher Order Filters for Grid Connected High Frequency Power Converters," Department of Electrical Engineering, IISc Bangalore.

Karshenas, H. R. and H. Saghafi, H. (2006). "Basic Criteria in Designing LCL Filters for Grid Connected Converters." Industrial Electronics, IEEE International Symposium. IEEE ISIE, July 9-12, Montreal, Canada, vol. 3, pp. 1996-2000.

Liserre, M.; Blaabjerg, F. and Hansen, S. (2005). "Design and control of an LCL- filter based three-phase active rectifier." Industry Applications, IEEE Transactions on vol. 41, no. 5, 1281-1291, 2005.

Pena-Alzola, R.; Liserre, M.; Blaabjerg, F.; Sebastian, R.; Dannehl, J. and Fuchs, F. W. (2013). "Analysis of the Passive Damping Losses in LCL – Filter – Based Grid Converters." IEEE Transactions on Power Electronics. Vol. 28 No. 6, pp. 2642 – 2646.

Reznik, A.; Godoy Simoes, M.; Al-Durra, A. and Muyeen, S. M. (2013). "LCL Filter Design and Performance Analysis for Grid Interconnected Systems," IEEE Transactions on Industry Applications, Vol. 50, No. 2, pp. 1225 – 1232.

Sarkar, A. (2015). "Modeling and Control of a Three Phase Voltage Source Inverter with an LCL Filter" MSc. Thesis, ARIZONA State University.